Dalton Transactions

ROYAL SOCIETY OF CHEMISTRY

PAPER

View Article Online
View Journal | View Issue

Cite this: *Dalton Trans.*, 2025, **54**, 11371

Attempted syntheses of ZnPhos-ruthenium complexes (ZnPhos = bis(2-diphenylphosphinophenyl)zinc)†

Amber M. Walsh, Ludovic J. Lewis, John P. Lowe, Mary F. Mahon and Michael K. Whittlesey *

Efforts to prepare Ru-ZnPhos complexes (ZnPhos = bis(2-diphenylphosphinophenyl)zinc) through *in situ* reactions of the bis-cyclometallated phosphine $RuZn_2$ complex $[Ru(PPh_3)(C_6H_4PPh_2)_2(ZnMe)_2]$ (**1**) with the N-Et and N-^{i}Pr substituted N-heterocyclic carbenes IEt_2Me_2 (1,3-diethyl-4,5-dimethylimidazol-2-ylidene) and $I^iPr_2Me_2$ (1,3-diisopropyl-4,5-dimethylimidazol-2-ylidene) gave instead the cycloruthenated/cyclozincated bimetallic species $[Ru(IEt_2Me_2')(C_6H_4PPh_2)(PPh_2(C_6H_4)Zn\{IEt_2Me_2\})H]$ (**5**; IEt_2Me_2' = cyclometallated IEt_2Me_2) and $[Ru(PPh_3)(C_6H_4PPh_2)(PPh(C_6H_4)_2Zn\{I^iPr_2Me_2\})H]$ (**7**) respectively, both of which feature new Zn-NHC bonds. An alternative approach involving substitution of free ZnPhos into ruthenium monodentate phosphine precursors proved marginally more successful. Heating $[Ru(PPh_3)_3(CO)H_2]$ with excess ZnPhos gave a tetrametallic species **13** comprised of a Ru centre coordinated to ZnPhos and two $ZnC_6H_4PPh_2$ ligands formed *via* Zn–C cleavage of two ZnPhos ligands. Substitution into the NHC analogue $[Ru(PPh_3)_2(IMe_4)(CO)H_2]$ (IMe_4 = 1,3,4,5-tetramethylimidazol-2-ylidene) was successful and generated the bridging dihydride complex $[Ru(ZnPhos)(IMe_4)(CO)(\mu\text{-}H)_2]$ (**14**).

Received 16th May 2025,
Accepted 24th June 2025

DOI: 10.1039/d5dt01160d

rsc.li/dalton

Introduction

Interest in pincer phosphine ligands ($R_2P\text{-}E\text{-}PR_2$, Fig. 1) stems from their highly tuneable stereoelectronic properties,[1–4] which in combination with their enhanced stability to the types of degradation reactions that affect monodentate phosphine ligands,[5] can result in favourable catalytic properties.[6]

Changing E from a non-metal to a Lewis acidic metal can alter the properties further by introduction of σ-accepting, Z-type character.[7] In contrast to the widespread studies of the group 13 elements Al, Ga and In,[8–16] investigations of pincer ligands with E = Zn, Cd and Hg remain sparse.[17–21] Whilst toxicity issues may explain the reluctance to develop Cd and Hg derivatives,[20,21] the relevance of Zn in conjunction with late transition metals[22] in reactions such as Pd-catalysed Negishi cross-coupling[23,24] suggests that $R_2P\text{-}Zn\text{-}PR_2$ pincers might offer worthwhile properties as ligands.[25]

We recently reported the serendipitous *in situ* formation of bis(2-diphenylphosphinophenyl)zinc (abbreviated as ZnPhos by analogy to bis(2-diphenylphosphinophenyl)ether, or DPEphos) complexes of ruthenium upon treating the bis-cyclometallated phosphine $RuZn_2$ complex $[Ru(PPh_3)(C_6H_4PPh_2)_2(ZnMe)_2]$ (**1**) with CO and the N-heterocyclic carbene IMe_4 (1,3,4,5-tetramethylimidazol-2-ylidene).[26] The resulting products, **2** and **3** respectively (Scheme 1), both reacted with H_2; the former photochemically to give the isolable bridging dihydride species **4**, the latter thermally to give terminal hydride **5** that existed in equilibrium with **3**. A short time later, Takaya's group[27] reported a synthetic route to the free ZnPhos ligand and utilised it in reactions with $Ru_3(CO)_{12}$ and $Pd(PPh_3)_4$ to give **2** and $[Pd(ZnPhos)(PPh_3)]$ (**6**) respectively (Scheme 1).

Prompted by the absence of any further reports of metal-ZnPhos complexes in the meantime, we set out to synthesise new Ru derivatives by (i) extending the *in situ* approach in Scheme 1 to NHCs other than IMe_4 and (ii) attempting to substitute free ZnPhos into labile Ru-PPh_3 precursors. We now show that *in situ* ZnPhos is limited to just IMe_4, while the sub-

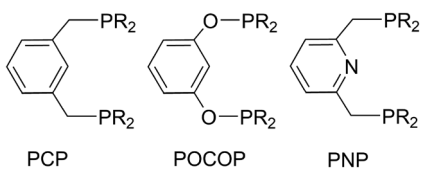

Fig. 1 Representative examples of P–E–P pincer ligands based on non-metallic E elements.

Department of Chemistry, University of Bath, Claverton Down, Bath BA2 7AY, UK. E-mail: m.k.whittlesey@bath.ac.uk

† Electronic supplementary information (ESI) available. CCDC 2409552–2409557. For ESI and crystallographic data in CIF or other electronic format see DOI: https://doi.org/10.1039/d5dt01160d

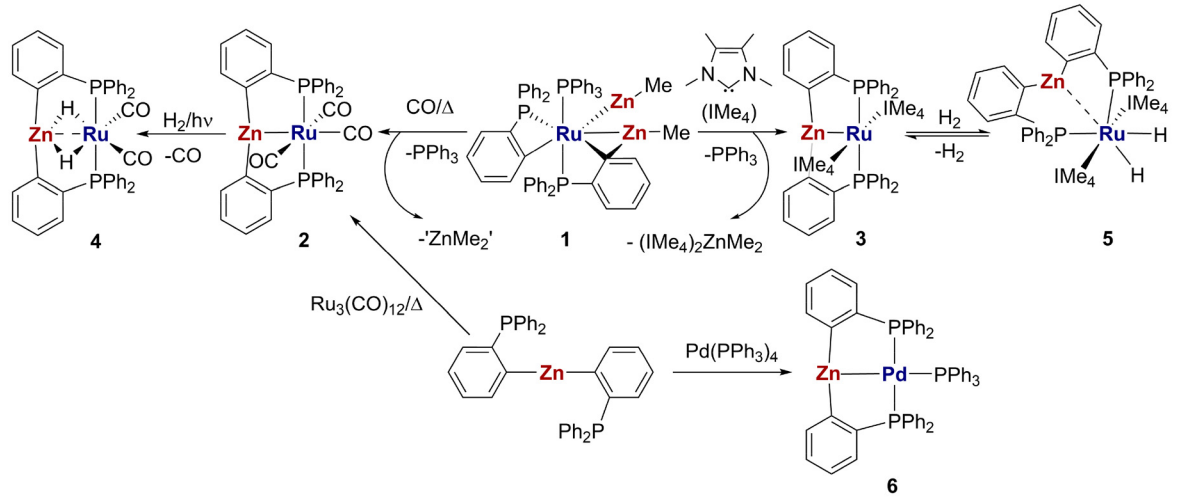

Scheme 1 Previously reported coordination chemistry of ZnPhos.[26,27]

stitution chemistry of the ligand illustrates a susceptibility to degradative Zn–C bond cleavage.

Results and discussion

Attempted *in situ* formation of Ru-ZnPhos complexes from 1 and NHCs

While the exact sequence of steps in Scheme 1 that transforms **1** to **3** is not known, the overall reaction entails elimination of PPh_3 and $ZnMe_2$ (the latter being trapped as the structurally characterised bis-carbene adduct $(IMe_4)_2ZnMe_2$) from **1**, insertion of Zn between two (2-diphenylphosphino)phenyl groups to generate the ZnPhos ligand and coordination of two molecules of IMe_4 to Ru.

Changing IMe_4 to IEt_2Me_2 (1,3-diethyl-4,5-dimethylimidazol-2-ylidene) did not result in Ru-ZnPhos formation, but gave instead the RuZn bimetallic complex **7** shown in Scheme 2. The structure of **7**, which was established by X-ray crystallography (Fig. 2), contained one intact IEt_2Me_2 ligand bound to Zn and a second IEt_2Me_2 ligand cyclometallated onto Ru (Ru1–C45 = 2.174(3) Å; Table 1).[28,29] The resulting hydride that was generated was located and freely refined in the X-ray structure as bridging between Ru and Zn; their separation of 2.5429(7) Å is well within the sum of the covalent radii (2.68 Å).[30] The X-ray structure also showed a phosphine ligand

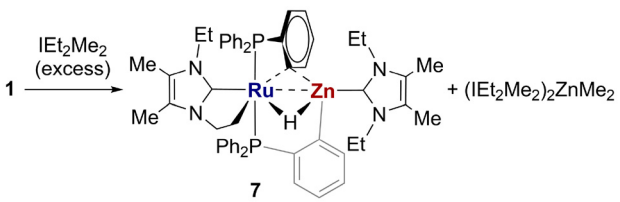

Scheme 2 Formation of the IEt_2Me_2 compound **7**.

(P2) cyclometallated onto Zn (Zn1–C18 = 2.013(3) Å), and a second (P1) cyclometallated mainly onto Ru, but with some interaction to Zn based on comparison of bond metrics (Scheme 3) to those reported for **1** and $ZnPh_2$.[26,31] The different rings sizes that arise from these interactions was clear from the $^{31}P\{^1H\}$ NMR spectrum, which showed one high (δ 83) and one low (δ −9) frequency resonance, indicative of the presence of five- and four-membered phosphorus ring chelates, respectively.[32,33]

As in the case of **3**, clean formation of **7** took place only in the presence of a significant excess of carbene. With 2 or 6 equivalents IEt_2Me_2, it formed a minor component alongside other hydride containing species,[34] whereas 10 equivalents of carbene gave **7** as the major product. Crude reaction mixtures contained *ca.* 25% of a second species, which we believe to be an isomer, although we were unable to find any conditions under which the yield of this product was increased.[35] Ultimately, **7** was isolated as orange-yellow microcrystalline material in 43% upon low temperature crystallisation from toluene/hexane, followed by manual separation away from colourless crystalline material assumed to be $(IEt_2Me_2)_2ZnMe_2$, by analogy to what was found during formation of **3** (Scheme 1).[36] No efforts were made to characterise or determine the yield of this side product.

Increasing the size of the carbene *N*-substituent further from N-Et to the N-^{i}Pr carbene $I^iPr_2Me_2$ (1,3-diisopropyl-4,5-dimethylimidazol-2-ylidene) gave **9** (Scheme 4), which was isolated in 58% yield as yellow crystals from benzene/hexane.[37] The X-ray structure (Fig. 2 and Table 1) confirmed that **9** contained a Zn-NHC ligand, but no Ru-NHC ligand, making it a direct analogue of the previously reported Zn(IMes) derivative **8** (IMes = 1,3-bis(2,4,6-trimethylphenyl)imidazol-2-ylidene; shown in Scheme 4 for comparison).[36] The X-ray structure of **9** showed three different types of phosphine ligands (one intact PPh_3, one cyclometallated onto Ru and the third with interaction from one of the phenyl rings to Ru and from a second

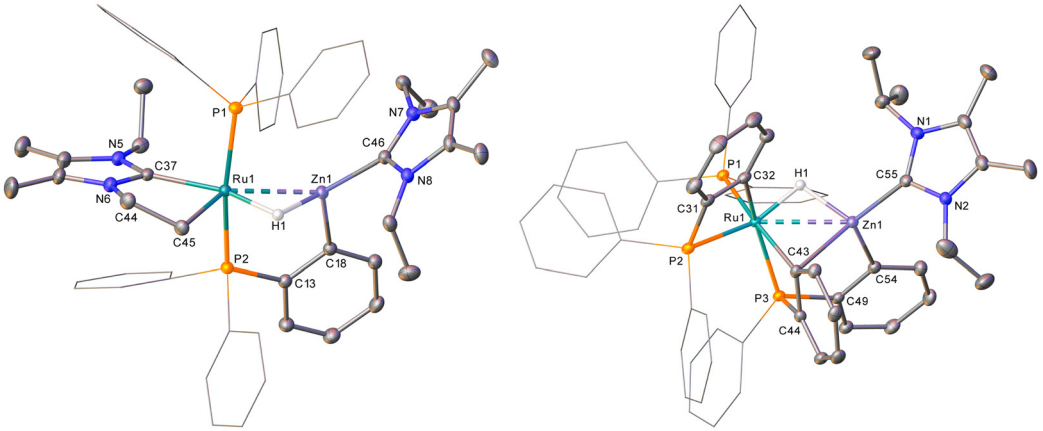

Fig. 2 Molecular structures of (left) **7** (one of the two molecules present in the structure) and (right) **9**. Ellipsoids are represented at 30% probability. In both cases, hydrogen atoms (hydride ligands excepted) are omitted for clarity. Solvent is also omitted for **7** for the same reason and peripheral substituents are depicted as wireframes for visual ease throughout.

Table 1 Selected bond lengths (Å) and angles (°) for compounds **7**, **9**, **10** and **11**

	7	**9**	**10**	**11**
Ru–Zn	2.5429(4)	2.6286(3)	2.6045(7)	2.5731(3)
Ru–P	Ru1–P1 2.3227(7) Ru1–P2 2.2937(7)	Ru1–P1 2.3141(5) Ru1–P2 2.3652(5) Ru–P3 2.3852(5)	Ru1–P1 2.3483(11) Ru1–P2 2.3745(12) Ru1–P3 2.3244(11)	Ru1–P1 2.3532(4) Ru1–P2 2.3404(4) Ru1–P3 2.3651(4)
Ru–C_{aryl}	2.221(3)	Ru1–C32 2.0852(19) Ru1–C43 2.1401(18)	Ru1–C12 2.121(4) Ru1–C30 2.114(5)	2.1072(17)
Ru–C_{other}	Ru1–C37 2.070(3) Ru1–C45 2.174(3)	—	—	—
Zn–C_{aryl}	Zn1–C18 2.013(3) Zn1–C35 2.311(3)	Zn1–C54 2.0197(19) Zn1–C48 2.393(2)	Zn1–C49 2.005(4) Zn1–C12 2.489(4)	Zn1–C38 1.9956(18)
Zn–C_{NHC}	2.035(3)	2.036(2)	2.053(4)	2.0321(18)
P–Ru–P	169.76(3)	P1–Ru1–P2 106.929(17) P2–Ru1–P3 102.352(17) P3–Ru1–P1 102.221(16)	167.43(4)	P1–Ru1–P2 100.859(16) P2–Ru1–P3 100.210(16) P3–Ru1–P1 110.112(16)

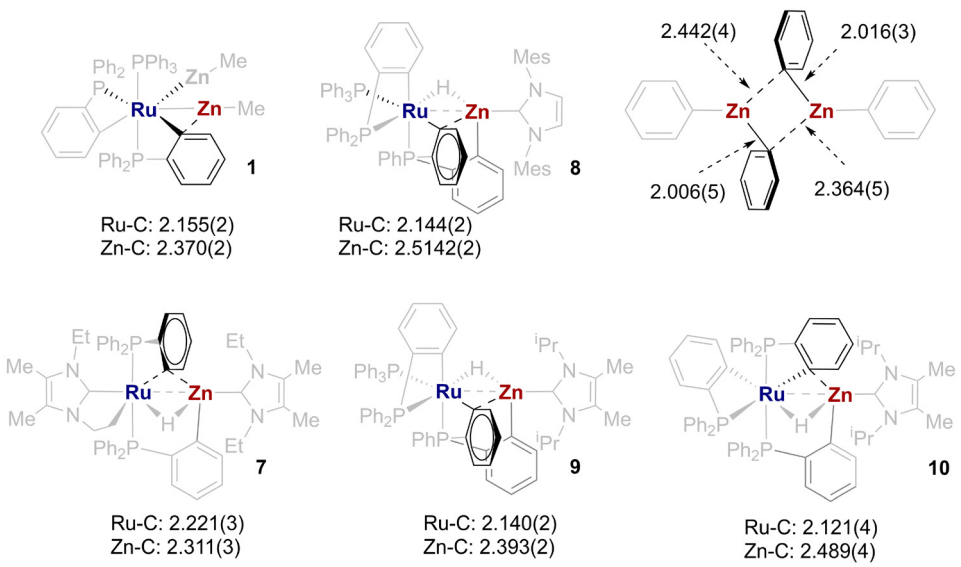

Scheme 3 Comparison of M–$C_{bridging\ aryl}$ distances (Å) in **1**,[36] **7–10** and $ZnPh_2$.[31]

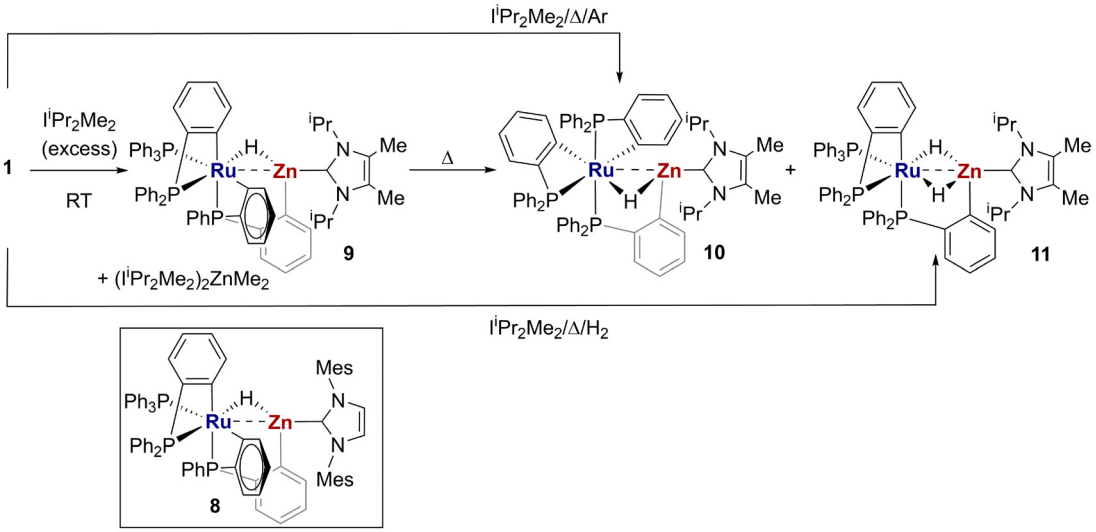

Scheme 4 Formation of the I^{i}Pr$_2$Me$_2$ compounds **9**–**11**. The previously reported IMes complex **8** is shown for comparison.[36]

ring to Zn) in a *fac*-geometry (Scheme 4). A hydride ligand bridging the Ru and Zn centres (separated by 2.6286(3) Å, slightly elongated in comparison to **7**) was again located and freely refined. The ^{1}H and ^{31}P NMR spectra of **9** were consistent with the X-ray data. Thus, the *trans* H-Ru-PPh$_2$(C$_6$H$_4$) geometry was confirmed by ^{1}H{selective-^{31}P} measurements, while the ^{31}P{^{1}H} NMR spectrum exhibited low frequency (δ −12, δ −24) resonances for the two cyclometallated phosphines, and a mid-frequency signal (δ 48) for the Ru-PPh$_3$ group.

For reasons that remain unclear, the formation of **9** required use of a much smaller excess of I^{i}Pr$_2$Me$_2$ (only 4 eq.) than the number of carbene equivalents used to generate **3** or **7**. Interestingly, even with 10 eq. I^{i}Pr$_2$Me$_2$, we observed no coordination of NHC onto Ru.

Broadness of the ^{1}H NMR methine signal led us to record spectra at 55 °C. While this yielded sharper spectra, it resulted over longer times in isomerisation of **9** to **10** (Scheme 4), which was formed alongside minor amounts of the bridging dihydride complex **11** (Scheme 4). We attribute formation of the latter to adventitious moisture. The identities of the two compounds were confirmed by X-ray crystallography and NMR spectroscopy following independent syntheses; **11** upon heating **1** with I^{i}Pr$_2$Me$_2$ at 70 °C under H$_2$, **10** by repeating the same process under argon. The X-ray structure of the latter (Fig. 3 and Table 1) revealed a *mer*-arrangement of three cyclometallated (two onto Ru, one onto Zn) phosphines, whereas **11** exhibited one intact PPh$_3$, one cycloruthenated ligand and one cyclozincated phosphine arranged in a *fac*-geometry. Despite the presence of the two bridging hydrides (which were both located in the X-ray structure; Fig. 3 and Table 1), the Ru···Zn distance was reduced to <2.60 Å. In the ^{1}H NMR spectrum of **11**, the two hydrides appeared as highly coupled resonances at δ −7.1 and δ −11.1, which were characterised as being *trans* to PPh$_3$ and *trans* to RuC$_6$H$_4$PPh$_2$ through ^{1}H{selective-^{31}P} NMR experiments.

Reactivity of ZnPhos with Ru–H precursors

Substitution reactions of free ZnPhos with Ru-PPh$_3$ complexes employed precursors used successfully in the synthesis of Ru(DPEphos) and related Ru(P–O–P) products.[38–40] Attempts to incorporate ZnPhos into [Ru(PPh$_3$)$_3$HCl] was thwarted by the insolubility of the latter in C$_6$H$_6$ and of the ligand in C$_6$H$_5$F. Use of CH$_2$Cl$_2$, in which [Ru(PPh$_3$)$_3$HCl] is fully soluble, resulted only in degradation of ZnPhos to PPh$_3$.[41] Although THF proved a viable solvent for reactions with both [Ru(PPh$_3$)$_3$HCl] and the carbonyl derivative [Ru(PPh$_3$)$_3$(CO)HCl], mixtures of products were formed in each case.

No reaction of the dihydride complex [Ru(PPh$_3$)$_3$(CO)H$_2$] with ZnPhos took place in C$_6$H$_6$ at room temperature, but heating at 80 °C overnight generated one main species which displayed three broad ^{31}P NMR resonances at δ 68, δ 60 and δ −17. Layering with hexane afforded deep-red crystals, which were identified by X-ray crystallography as the unexpected RuZn$_3$ tetrametallic complex **13** shown in Scheme 5. The X-ray structure (Fig. 4) revealed a 7-coordinate Ru centre coordinated to ZnPhos and CO ligands as well as to the Zn atom (Zn2) of a ZnC$_6$H$_4$PPh$_2$ moiety (Ru1–Zn2 = 2.5129(6) Å). The phosphorus atom was bound to the Zn (Zn3) of the second ZnC$_6$H$_4$PPh$_2$ ligand, which then completed the coordination sphere of Ru being κ^2-Zn,P bonded (Ru1–Zn3 = 2.6386(5) Å, Ru1–P4 = 2.4296(9) Å). Selected metrics for the structure are given in Table 2.

Formation of the two ZnC$_6$H$_4$PPh$_2$ groups arises through Zn–C cleavage of two ZnPhos ligands. In turn, this also generates 2 eq. of –C$_6$H$_4$PPh$_2$, which upon combination with two Ru–H ligands, yields two of the five equivalents of PPh$_3$ (three lost from [Ru(PPh$_3$)$_3$(CO)H$_2$]) generated overall in the reaction, as established by a ^{31}P{inverse-gated ^{1}H} NMR measurement.

Crystalline **13** failed to redissolve in benzene but did dissolve in THF, yielding a ^{31}P{inverse-gated ^{1}H} NMR spectrum

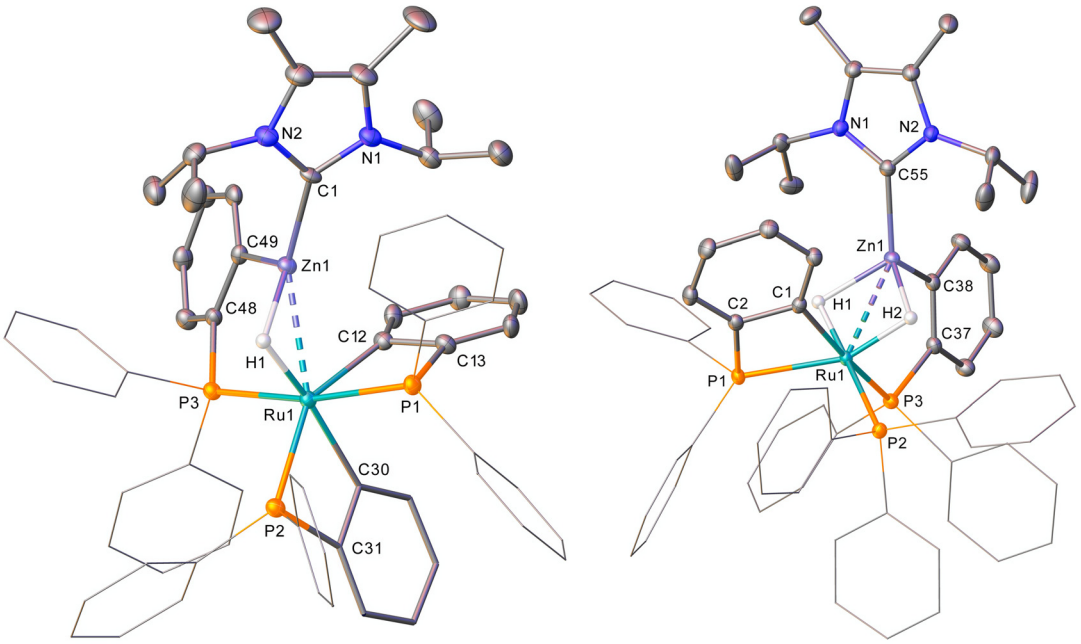

Fig. 3 Molecular structures of (left) **10** and (right) **11**. Ellipsoids are represented at 30% probability. In both cases, hydrogen atoms (hydride ligands excepted) are omitted for clarity. Solvent, in **11**, is similarly absent. Peripheral substituents are depicted as wireframes, also for visual ease.

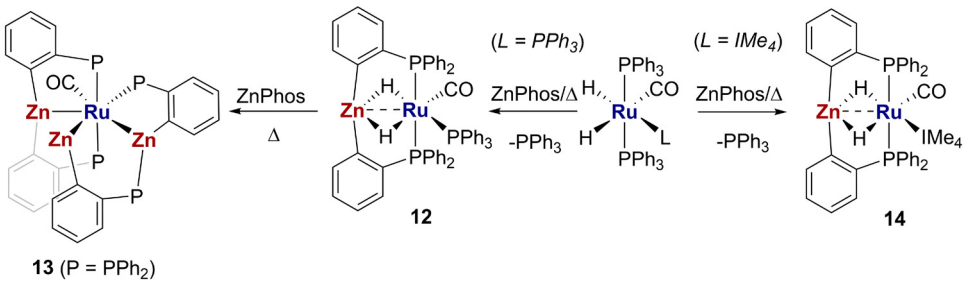

Scheme 5 Reactivity of $[Ru(PPh_3)_2(L)(CO)H_2]$ (L = PPh_3, IMe_4) with ZnPhos.

comprised of a 1 : 2 : 1 ratio of three resonances at similar chemical shifts to those in the crude reaction mixture, but now resolved into triplets (albeit still quite broad), all with J_{PP} splitting of just 6 Hz. Removal of THF gave a red residue that did now redissolve in C_6D_6 to give a spectrum identical to that of the crude material.

The triplet multiplicity of phosphorus P3 (Fig. 4) appears to be at odds with the solid-state structure, as is the size of the P, P-couplings, which are significantly smaller than *cis* P–Ru–P J_{PP} values which are typically *ca.* 20 Hz.[42,43] These findings are suggestive of fluxionality in the system; indeed, cooling to very low temperature (−85 °C) broadened significantly the signal at *ca.* δ 60; only three resonances were observed at all temperatures. There was also noticeable shift ($\Delta\delta$) of +0.5 ppm in the lowest frequency resonance upon cooling, as well as an even more pronounced $\Delta\delta$ of −2 ppm in the signal for free PPh_3 in the sample; both observations further support one or more processes of fluxionality/exchange. Higher temperature spectra were compromised by degradation of starting material resonances and an increase in free PPh_3, a process that also took place in solution even at room temperature over time.

In light of the X-ray structure, solid-state $^{31}P\{^1H\}$ CPMAS NMR spectra of crystalline **13** were measured. These also revealed three resonances at *ca.* δ 67, δ 55 and δ −14, along with a signal for free PPh_3 (*ca.* δ −7, proven by addition of PPh_3, which was then used as an internal reference)[44] and a broad resonance of unknown origin at δ −5. ^{31}P spin-diffusion measurements showed correlations between all three resonances, confirming they originated from within the same molecule. This was supported by a ^{31}P-detected ^1H T_1 measurement. As protons in the same molecule should show the same T_1 (the result of dipolar coupling), the ^{31}P signals associated with each molecule should then show the same ^1H T_1 value; this was what was observed (Table S1;† the small discrepancies are attributed to issues with fittings signals of low intensity).[45] The different ^1H T_1 associated with the broad −5 ppm signal,

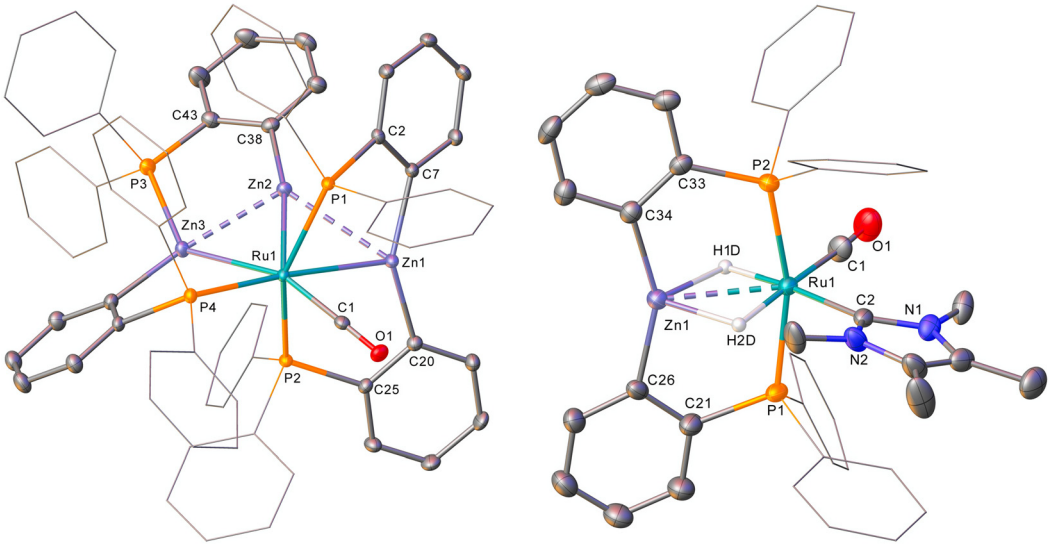

Fig. 4 Plots depicting (left) the structure of **13** and (right) one of the four molecules present in the structure of **14**. Ellipsoids are shown at 30% probability. Solvent in **13** and hydrogen atoms in both structures (hydride ligands excepted) have been omitted for clarity. Peripheral substituents are depicted as wireframes, also for visual ease.

Table 2 Selected bond lengths (Å) and angles (°) for compounds **13** and **14**

	13	**14** [a]
Ru–Zn1	2.6544(5)	2.6437(15)
Ru–Zn2	2.5129(6)	—
Ru–Zn3	2.6386(5)	—
Ru–P1	2.3784(8)	2.329(3)
Ru–P2	2.3561(8)	2.319(2)
Ru–P4	2.4296(9)	—
Ru–C_{other}	Ru1–C1: 1.881(4)	Ru1–C1: 1.886(12) Ru1–C2: 2.137(9)
Zn–P	Zn3–P3: 2.4885(11)	—
Zn–Zn	Zn1–Zn2: 2.7815(7) Zn2–Zn3: 2.5371(7)	—
Zn–C_{aryl}	Zn1–C7: 1.987(3) Zn1–C20: 1.961(4) Zn2–C38: 1.980(4) Zn3–C56: 1.972(4)	Zn1–C26: 1.989(7) Zn1–C34: 1.990(7)
P1–Ru–P2	151.66(3)	167.07(10)
P1–Ru–P4	104.59(3)	—
P2–Ru–P4	103.53(3)	—

[a] Data are for one of the four molecules of the compound in the unit cell.

together with the absence of cross-peaks to this in the ^{31}P spin diffusion experiment, are consistent with this resonance being from a different species.

When the formation of **13** was followed by $^{31}P\{^{1}H\}$ NMR spectroscopy, free PPh_3, together with signals attributed to the substitution product $[Ru(ZnPhos)(PPh_3)(CO)H_2]$ (**12**, Scheme 5), appeared within 1 h. Full consumption of $[Ru(PPh_3)_3(CO)H_2]$ took place over *ca.* 3–4 h, leaving **13** as the major solution component after *ca.* 5 h.[47] Under more concentrated conditions, **13** precipitated directly from solution, leaving a filtrate comprised, in part, of **12**. Heating this with ZnPhos gave **13**, consistent with **12** being a precursor to the final tetrametallic product (Scheme 5). The exact structure of **12** (it is shown with bridging hydrides in Scheme 5 based on the similarity of the ^{1}H NMR hydride resonances to those of **4** and **14** (*vide infra*)) and the mechanism of conversion to **13** remain unknown, although it is tempting to suggest that an intramolecular attack of Ru–H on a Zn–C bond of coordinated ZnPhos is involved.[46] Attempts to generate just **12** *via* sequentially adding up to 4 equivalents of ZnPhos to $[Ru(PPh_3)_3(CO)H_2]$ gave **12** as part of a mixture together with unreacted $[Ru(PPh_3)_3(CO)H_2]$ or tetrametallic **13**.

In contrast to the degradative reaction with $[Ru(PPh_3)_3(CO)H_2]$, ZnPhos (2 eq.) afforded the intact substitution product $[Ru(ZnPhos)(IMe_4)(CO)(\mu\text{-}H)_2]$ (**14**, Scheme 5) in 32% isolated yield after heating with $[Ru(PPh_3)_2(IMe_4)(CO)H_2]$ at 40 °C for 24 h. This time could be cut to just 6 h by increasing the temperature to 70 °C, allowing us to exclude elevated temperatures as being responsible for the Zn–C cleavage that yields **13**. Based on the proposed intramolecular attack mooted above, it may be that the change from PPh_3 to the strongly donating IMe_4 ligand in **14** disfavours such a process.

The X-ray crystal structure of **14** (Fig. 4) confirmed the presence of bridging hydrides analogous to the arrangement in **4** (Scheme 1). Four molecules were present in the unit cell of **14**, with the Ru···Zn separation ranging from 2.6422(14)–2.6672(15) Å, considerably shorter than that in **4** (2.8080(9) and 2.8184(9) Å, 2 molecules in the unit cell). As shown in Scheme 1, a contrasting structure with terminal hydrides was found for the bis-IMe_4 derivative **5**, which computational studies showed relates to the kinetics of the addition of H_2 to $[Ru(ZnPhos)(IMe_4)_2]$ (**3**).[27] The bridging hydride structure of **14** (and, indeed, **12**) may result from the hydride ligands being present in the precursor, rather than formed through addition of H_2.

Conclusions

Two approaches have been used in an effort to synthesise new ZnPhos complexes of ruthenium. Following on from our previous report of the formation of [Ru(ZnPhos)(IMe_4)$_2$] (**3**, Scheme 2) from [Ru(PPh_3)($C_6H_4PPh_2$)$_2$($ZnMe_2$)$_2$] (**1**) and IMe_4, we have found that the latter appears to be the only NHC able to bring about *in situ* ZnPhos formation from **1**, with both *N*-ethyl and *N*-isopropyl substituted carbenes showing behaviour analogous to IMes in giving instead Ru···Zn(NHC) containing products. Substitution of free ZnPhos into labile Ru precursors has proven to be slightly more successful, giving [Ru(ZnPhos)(IMe_4)(CO)(μ-H)$_2$] (**14**) from the NHC precursor [Ru(PPh_3)$_2$(IMe_4)(CO)H_2]. However, with the all-phosphine complex [Ru(PPh_3)$_3$(CO)H_2], Zn–C cleavage takes place to give the tetrametallic species **13**, revealing a vulnerability of ZnPhos to degradative processes that may ultimately limit its value for catalysis. Whilst disappointing, we feel that this still represents a valuable observation of the type often overlooked.[48]

Experimental section

All manipulations were carried out at room temperature under argon using standard Schlenk, high vacuum and glovebox techniques using dry and degassed solvents. C_6D_6, $C_6D_5CD_3$ and THF-d_8 were vacuum transferred from potassium. NMR spectra were recorded on Bruker Avance 400 and 500 MHz NMR spectrometers and referenced as follows: C_6D_6 (δ_H 7.15; δ_C 128.0), $C_6D_5CD_3$ (δ_H 2.09; δ_C 20.4) and THF-d_8 (δ_H 3.58; δ_C 25.4). $^{31}P\{^1H\}$ spectra were referenced externally to 85% H_3PO_4 at δ 0. Coupling constants are defined using $^xJ_{AB}$ nomenclature only where there is absolute certainty in assignments; vt = virtual triplet. The ^{31}P CPMAS and spin diffusion experiments and the ^{31}P-detected ^{1}H T_1 measurement of solid **13** were acquired on a Bruker Avance 500 MHz spectrometer using a 4 mm iProbe CPMAS. The spin diffusion experiment was carried out using a DARR (Dipolar Assisted Rotational Resonance) pulse sequence; the T_1 measurement using an inversion recovery method. IR spectra were recorded on a Bruker ALPHA ATR-IR spectrometer. Elemental analyses were performed by Elemental Microanalysis Ltd, Okehampton, Devon, U.K. Literature routes were used for the synthesis of [Ru(PPh_3)($C_6H_4PPh_2$)$_2$($ZnMe_2$)$_2$] (**1**),[26] [Ru(PPh_3)$_3$HCl],[49] [Ru(PPh_3)$_3$(CO)HCl],[50] [Ru(PPh_3)$_3$(CO)H_2],[51] $I^iPr_2Me_2$ and IEt_2Me_2.[52] ZnPhos was prepared according to the literature,[27] albeit starting from 2-(diphenylphosphino)phenylboronate, which was prepared from 1,2-dibromobenzene.[53,54]

Synthesis and characterisation of 7

A J. Youngs resealable ampoule was charged with **1** (50 mg, 0.05 mmol), IEt_2Me_2 (72 mg, 0.5 mmol) and benzene (3 mL) and the solution stirred at room temperature overnight.‡ After filtration, the filtrate was reduced to dryness and the residue recrystallised from toluene/hexane at −37 °C to afford a mixture of orange-yellow crystals of the product and colourless crystals of what are assumed to be $(IEt_2Me_2)_2ZnMe_2$, which were separated manually. Yield: 21 mg (43%). ^{1}H NMR: δ_H (500 MHz, $C_6D_5CD_3$, 233 K): 8.28 (br t, $^3J_{HH}$ = 7.0 Hz, 2H, Ar), 8.11–8.02 (br m, 4H, Ar), 7.71 (br m, 1H, Ar), 7.53 (vbr s, 1H, Ar), 7.32 (br t, $^3J_{H,H}$ = 6.9 Hz, 1H, Ar), 7.27 (t, $^3J_{H,H}$ = 7.4 Hz, 2H, Ar), 6.98–6.86 (m, 5H, Ar), 6.85–6.68 (m, 6H, Ar), 6.57 (br t, $^3J_{H,H}$ = 8.2 Hz, 1H, Ar),* 4.55 (m, 1H, NC*H*H), 3.86 (t, $^3J_{H,H}$ = 9.5 Hz, 1H, RuCH$_2$C*H*H), 3.72 (m, 1H, NC*H*H), 3.16 (m, 1H, NC*H*H), 3.00 (m, 1H, RuCH$_2$CH*H*), 2.58 (vbr m, 1H, RuC*H*HCH$_2$), 2.42 (m, 1H, NC*H*H), 2.16 (m, 1H, NC*H*H), 1.65–1.59 (overlapping m + s, 4H, NCH*H* + NC=CC*H*$_3$),† 1.57 (s, 3H, NC=CC*H*$_3$), 1.32–1.19 (overlapping m + s, 7H, RuCH*H*CH$_2$ + NC=CC*H*$_3$),† 1.07 (t, $^3J_{HH}$ = 7.1 Hz, 3H, NCH$_2$C*H*$_3$), 0.87 (t, $^3J_{H,H}$ = 7.1 Hz, 3H, NCH$_2$C*H*$_3$), 0.46 (t, $^3J_{H,H}$ = 6.9 Hz, 3H, NCH$_2$C*H*$_3$), −6.78 (br dd, $^2J_{H,P}$ = 17.4 Hz, $^2J_{H,P}$ = 15.1 Hz, 1H, Ru*H*). *The remaining aromatic resonances are assumed to be obscured by solvent signals. †Established by ^{1}H COSY. $^{31}P\{^1H\}$ NMR: δ_P (202 MHz, $C_6D_5CD_3$, 233 K): 83.0 (d, $^2J_{P,P}$ = 298 Hz), −8.6 (d, $^2J_{P,P}$ = 298 Hz). Selected $^{13}C\{^1H\}$ DEPTQ NMR: δ_C (126 MHz, $C_6D_5CD_3$, 233 K): 192.4 (br t, $^2J_{C,P}$ = 11 Hz, Ru–C_{NHC}), 177.2 (s, Zn–C_{NHC}), 53.3 (s, N*C*H$_2$CH$_2$Ru), 42.5 (s, N*C*H$_2$CH$_3$), 41.7 (s, N*C*H$_2$CH$_3$), 40.7 (s, N*C*H$_2$CH$_3$), 17.6 (s, NCH$_2$*C*H$_3$), 16.9 (s, NCH$_2$*C*H$_3$), 15.5 (s, NCH$_2$*C*H$_3$), 9.6 (s, NC=C*C*H$_3$), 9.3 (s, NC=C*C*H$_3$), 7.7 (s, NC=C*C*H$_3$), 7.6 (s, NC=C*C*H$_3$), 3.9 (br s, NCH$_2$*C*H$_2$Ru). Elemental analysis. Found: C, 59.85; H, 6.18; N, 5.90. $C_{54}H_{60}N_4P_2ZnRu$ requires C, 65.28; H, 6.09; N, 5.64. Multiple attempts repeatedly gave low %*C* values. ‡Crude reaction mixtures showed *ca.* 25% of a second hydride containing species, which we propose is an isomer of **7**. Selected ^{1}H NMR: δ_H (500 MHz, C_6D_6, 298 K): −8.49 (dd, $^2J_{H,P}$ = 51.7 Hz, $^2J_{H,P}$ = 4.0 Hz, 1H, Ru–*H*). $^{31}P\{^1H\}$ NMR: δ_P (202 MHz, C_6D_6, 298 K): −5.8 (d, $^2J_{P,P}$ = 20 Hz), −15.4 (d, $^2J_{P,P}$ = 20 Hz).

Synthesis and characterisation of 9

A J. Youngs resealable ampoule was charged with a benzene (3 mL) solution of **1** (50 mg, 0.05 mmol) and $I^iPr_2Me_2$ (43 mg, 0.24 mmol) and the mixture stirred overnight at room temperature. Following filtration, the filtrate was reduced to dryness, washed with hexane (3 mL) and recrystallised from benzene and hexane to yield yellow crystals of **9**. Yield: 35 mg (58%). ^{1}H NMR: δ_H (400 MHz, C_6D_6, 298 K): 7.68 (t, J = 7.8 Hz, 2H, Ar), 7.57 (d, J = 6.4 Hz, 1H, Ar), 7.51–7.34 (br, 11H, Ar), 7.28–7.18 (br, 4H, Ar), 7.13–7.02 (br, 4H, Ar),* 7.01–6.78 (br m, 15 H, Ar), 6.78–6.64 (m, 3H, Ar), 6.55 (t, J = 7.2 Hz, 1H, Ar), 6.44 (t, J = 7.2 Hz, 1H, Ar), 4.24 (br s, 2H, C*H*(CH$_3$)$_2$), 1.50 (s, 6H, NC=C(C*H*$_3$)), 0.96 (overlapping d, $^3J_{H,H}$ = 6.8 Hz, 12H, CH(C*H*$_3$)$_2$), −9.31 (br ddd, $^2J_{H,P}$ = 53.5 Hz, $^2J_{H,P}$ = 24.5 Hz, $^2J_{H,P}$ = 2.6 Hz, 1H, Ru–*H*). *Partially overlapped with resonance for C_6D_5H. ^{1}H NMR: δ_H (400 MHz, $C_6D_5CD_3$, 328 K): 7.63 (br t, J = 7.6 Hz, 2H, Ar), 7.44 (br d, J = 6.4 Hz, 1H, Ar), 7.39–7.31 (br, 9H, Ar), 7.28–7.16 (br, 4H, Ar), 6.96–6.64 (br, 17 H, Ar), 6.78–6.64 (m, 3 H, Ar), 6.54 (br m, 1H, Ar), 6.45 (br t, J = 7.2 Hz, 1H, Ar), 6.36 (br t, J = 7.3 Hz, 1H, Ar),* 4.23 (sept, $^3J_{H,H}$ = 8.8 Hz, 2H, C*H*(CH$_3$)$_2$), 1.65 (s, 6H, NC=C(C*H*$_3$)), 1.02–0.98

(overlapping d, $^{3}J_{H,H}$ = 6.8 Hz, 12H, CH(CH_3)$_2$), −9.51 (ddd, $^{2}J_{H,P}$ = 52.9 Hz, $^{2}J_{H,P}$ = 24.5 Hz, $^{2}J_{H,P}$ = 3.1 Hz, 1H, Ru–*H*). *The remaining aromatic resonances are assumed to be obscured by solvent signals. $^{31}P\{^{1}H\}$ NMR: δ_P (162 MHz, C_6D_6, 298 K): 48.2 (t, $^{2}J_{P,P}$ = 25 Hz), −11.9 (dd, $^{2}J_{P,P}$ = 25 Hz, $^{2}J_{P,P}$ = 16 Hz), −23.9 (dd, $^{2}J_{P,P}$ = 25 Hz, $^{2}J_{P,P}$ = 16 Hz). $^{13}C\{^{1}H\}$ NMR: δ_C (101 MHz, C_6D_6, 298 K): 177.8 (ddd, $J_{C,P}$ = 67 Hz, $J_{C,P}$ = 12 Hz, $J_{C,P}$ = 6 Hz, Ar), 176.2 (br dm, $J_{C,P}$ = 5 Hz, Zn–C_{NHC}), 170.3 (br dm, $J_{C,P}$ = 42 Hz, Ar), 168.5 (d, $J_{C,P}$ = 61 Hz, Ar), 165.4 (dd, $J_{C,P}$ = 57 Hz, $J_{C,P}$ = 12 Hz, Ar), 153.4 (dd, $J_{C,P}$ = 47 Hz, $J_{C,P}$ = 5 Hz, Ar), 149.0 (d, $J_{C,P}$ = 35 Hz, Ar), 142.7 (br dm, $J_{C,P}$ = 29 Hz, Ar), 142.0 (d, $J_{C,P}$ = 10 Hz, Ar), 140.6 (d, $J_{C,P}$ = 20 Hz, Ar), 140.5 (d, $J_{C,P}$ = 21 Hz, Ar), 137.2 (d, $J_{C,P}$ = 23 Hz, Ar), 137.0 (d, $J_{C,P}$ = 9 Hz, Ar), 135.8 (d, $J_{C,P}$ = 25 Hz, Ar), 134.5 (d, $J_{C,P}$ = 13 Hz, Ar), 134.4 (d, $J_{C,P}$ = 12 Hz, Ar), 133.8 (d, $J_{C,P}$ = 10 Hz, Ar), 132.4 (d, $J_{C,P}$ = 10 Hz, Ar), 128.8 (m, Ar), 128.5 (s, Ar), 127.4 (d, $J_{C,P}$ = 8 Hz, Ar), 127.2 (d, $J_{C,P}$ = 8 Hz, Ar), 126.2 (d, $J_{C,P}$ = 5 Hz, Ar), 125.9 (s, Ar), 125.4 (s, NC═*C*CH$_3$), 125.3 (m, Ar), 122.5 (s, Ar), 119.5 (d, $J_{C,P}$ = 8 Hz, Ar), 53.3 (s, N*C*H(CH$_3$)$_2$), 22.4 (s, NCH(*C*H$_3$)$_2$), 22.1 (s, NCH (*C*H$_3$)$_2$), 9.8 (s, NC═C*C*H$_3$). Elemental analysis. Found: C, 69.14; H, 5.72; N, 2.56. $C_{65}H_{63}N_2P_3ZnRu$ requires C, 68.99; H, 5.61; N, 2.48.

Synthesis and characterisation of 10

Using the same masses/volumes as for **9**, the contents of the ampoule were heated at 70 °C for 15 h. After filtration/washing as per **9**, the residue was crystallised from benzene/hexane to give 30 mg (50%) of **10** as yellow crystals. ^{1}H NMR: δ_H (400 MHz, C_6D_6, 298 K): 8.44 (t, J = 8.5 Hz, 2H, Ar), 8.14 (dt, J = 19.3 Hz, J = 8.2 Hz, 4H, Ar), 7.78 (dd, J = 7.2 Hz, J = 5.1 Hz, 1H, Ar), 7.59–7.50 (m, 3H, Ar), 6.97 (app quart, J = 7.6 Hz, 3H, Ar), 6.93–6.49 (br m, 19H, Ar), 6.26 (t, J = 8.5 Hz, 2H, Ar),* 4.73 (br sept, $^{3}J_{H,H}$ = 6.3 Hz, 1H, CH(CH_3)$_2$), 2.47 (sept, $^{3}J_{H,H}$ = 6.4 Hz, 1H, CH(CH_3)$_2$), 1.57 (d, $^{3}J_{H,H}$ = 6.4 Hz, CH*Me*$_2$, 3H), 1.56 (s, NC═CC*H*$_3$, 3H), 1.49 (d, $^{3}J_{H,H}$ = 6.4 Hz, CH*Me*$_2$, 3H), 1.43 (s, NC═CC*H*$_3$, 3H), 0.79 (d, $^{3}J_{H,H}$ = 6.5 Hz, CH*Me*$_2$, 3H), 0.09 (d, $^{3}J_{H,H}$ = 6.4 Hz, CH*Me*$_2$, 3H), −5.68 (td, $^{2}J_{H,P}$ = 12.7 Hz, $^{2}J_{H,P}$ = 6.7 Hz, 1H, Ru*H*). *The remaining aromatic signals are obscured by C_6D_5H. $^{31}P\{^{1}H\}$ NMR: δ_P (162 MHz, C_6D_6, 298 K): 78.2 (d, $^{2}J_{P,P}$ = 288 Hz, $^{2}J_{P,P}$ = 22 Hz), −14.9 (dd, $^{2}J_{P,P}$ = 288 Hz, $^{2}J_{P,P}$ = 26 Hz), −20.0 (dd, $^{2}J_{P,P}$ = 26 Hz, $^{2}J_{P,P}$ = 22 Hz). $^{13}C\{^{1}H\}$ NMR: δ_C (101 MHz, C_6D_6, 298 K): 179.5 (dt, $J_{C,P}$ = 10 Hz, $J_{C,P}$ = 6 Hz, Ar), 179.4 (s, Zn–C_{NHC}), 175.3 (dd, $J_{C,P}$ = 70 Hz, $J_{C,P}$ = 3 Hz, Ar), 163.8 (ddd, $J_{C,P}$ = 53 Hz, $J_{C,P}$ = 7 Hz, $J_{C,P}$ = 4 Hz, Ar), 158.0 (dd, $J_{C,P}$ = 43 Hz, $J_{C,P}$ = 5 Hz, Ar), 152.0 (dd, $J_{C,P}$ = 45 Hz, $J_{C,P}$ = 3 Hz, Ar), 151.0 (d, $J_{C,P}$ = 54 Hz, Ar), 144.2 (dd, $J_{C,P}$ = 18 Hz, $J_{C,P}$ = 5 Hz, Ar), 142.6 (dd, $J_{C,P}$ = 23 Hz, $J_{C,P}$ = 3 Hz, Ar), 140.8 (d, $J_{C,P}$ = 31 Hz, Ar), 139.5 (d, $J_{C,P}$ = 17 Hz, Ar), 138.4 (d, $J_{C,P}$ = 22 Hz, Ar), 137.8 (d, $J_{C,P}$ = 27 Hz, Ar), 137.3 (d, $J_{C,P}$ = 33 Hz, Ar), 136.7 (d, $J_{C,P}$ = 5 Hz, Ar), 136.4 (d, $J_{C,P}$ = 12 Hz, Ar), 135.2 (br d, $J_{C,P}$ = 5 Hz, Ar), 135.0 (br d, $J_{C,P}$ = 14 Hz, Ar), 134.2 (d, $J_{C,P}$ = 9 Hz, Ar), 133.9 (d, $J_{C,P}$ = 4 Hz, Ar), 132.8 (d, $J_{C,P}$ = 9 Hz, Ar), 132.7 (d, $J_{C,P}$ = 10 Hz, Ar), 130.2 (d, $J_{C,P}$ = 8 Hz, Ar), 129.6 (br s, Ar), 128.8 (br s, Ar), 128.5 (s, Ar), 127.4 (d, $J_{C,P}$ = 8 Hz, Ar), 127.2 (d, $J_{C,P}$ = 22 Hz, Ar), 127.0–126.3 (m, Ar), 125.2 (s, NC═*C*CH$_3$), 125.0 (br m, Ar), 124.5 (br s, Ar), 123.7 (s, NC═*C*CH$_3$), 120.9 (br s, Ar), 120.1 (br s, Ar), 53.8 (s, N*C*H (CH$_3$)$_2$), 51.5 (s, N*C*H(CH$_3$)$_2$), 23.5 (s, NCH(*C*H$_3$)$_2$), 22.8 (s, NCH (*C*H$_3$)$_2$), 22.7 (s, NCH(*C*H$_3$)$_2$), 21.4 (s, NCH(*C*H$_3$)$_2$), 10.0 (s, NC═*C*CH$_3$), 9.2 (s, NC═C*C*H$_3$). Elemental analysis. Found: C, 65.28; H, 5.07; N, 2.37. $C_{65}H_{63}N_2P_3ZnRu$ requires C, 68.99; H, 5.61; N, 2.48. Multiple attempts repeatedly gave low %*C* values.

Synthesis and characterisation of 11

Using the same masses/volumes as for **9**, the ampoule was freeze–pump–thaw degassed three times, placed under 1 atm H_2 and stirred at room temperature overnight. After filtration/washing as per **9**, the residue was crystallised from benzene/hexane to give 26 mg (43%) of yellow crystals of **11**. ^{1}H NMR: δ_H (400 MHz, C_6D_6, 318 K): 8.07 (d, J = 6.7 Hz, 1H, Ar), 7.98 (t, J = 8.1 Hz, 2H, Ar), 7.81 (br t, J = 8.5 Hz, 2H, Ar), 7.42–7.17 (m, 9H, Ar),* 7.09–6.97 (m, 6H, Ar), 6.97–6.75 (m, 13H, Ar), 6.73–6.56 (m, 6H, Ar), 4.37 (sept, $^{3}J_{H,H}$ = 6.8 Hz, 2H, CH (CH_3)$_2$), 1.51 (s, NC═CC*H*$_3$, 6H), 1.29–1.12 (br, CH*Me*$_2$, 6H), 1.04 (br s, CH*Me*$_2$, 6H), −7.10 (dddd, $^{2}J_{H,P}$ = 59.1 Hz, $^{2}J_{H,P}$ = 20.2 Hz, $^{2}J_{H,P}$ = 15.6 Hz, $^{2}J_{H,H}$ = 7.3 Hz, 1H, Ru*H*),† −11.12 (dm, $^{2}J_{H,P}$ = 51.7 Hz, $^{2}J_{H,P}$ = 11.7 Hz, $^{2}J_{H,P}$ = 9.4 Hz, $^{2}J_{H,H}$ = 7.3 Hz, 1H, Ru*H*).† *The remaining aromatic signals are obscured by C_6D_5H. †Values determined by $^{1}H\{$selective-$^{31}P\}$ measurements. $^{31}P\{^{1}H\}$ NMR: δ_P (202 MHz, C_6D_6, 298 K): 63.7 (dd, $^{2}J_{P,P}$ = 20 Hz, $^{2}J_{P,P}$ = 16 Hz), 57.6 (t, $^{2}J_{P,P}$ = 20 Hz), −19.5 (dd, $^{2}J_{P,P}$ = 20 Hz, $^{2}J_{P,P}$ = 16 Hz). $^{13}C\{^{1}H\}$ NMR: δ_C (101 MHz, C_6D_6, 318 K): 176.9 (br m, Zn–C_{NHC}), 175.7–174.1 (overlapping m, Ar),* 155.5 (d, $J_{C,P}$ = 47 Hz, Ar), 154.0 (d, $J_{C,P}$ = 49 Hz, Ar), 145.3 (dd, $J_{C,P}$ = 18 Hz, $J_{C,P}$ = 3 Hz, Ar), 145.0 (d, $J_{C,P}$ = 18 Hz, Ar), 142.8 (d, $J_{C,P}$ = 28 Hz, Ar), 141.3 (d, $J_{C,P}$ = 23 Hz, Ar), 140.4 (d, $J_{C,P}$ = 30 Hz, Ar), 140.0 (d, $J_{C,P}$ = 12 Hz, Ar), 135.1 (br, Ar), 133.1 (br, Ar), 132.6 (d, $J_{C,P}$ = 11 Hz, Ar), 127.5 (br s, Ar), 127.1–126.7 (overlapping m, Ar), 126.3 (s, Ar), 125.0 (d, $J_{C,P}$ = 4 Hz, Ar), 124.6 (s, NC═*C*CH$_3$), 124.3 (d, $J_{C,P}$ = 5 Hz, Ar), 119.4 (d, $J_{C,P}$ = 8 Hz, Ar), 51.8 (s, N*C*H(CH$_3$)$_2$), 22.8 (s, NCH(*C*H$_3$)$_2$), 9.2 (s, NC═C*C*H$_3$). Elemental analysis. Found: C, 68.88; H, 6.13; N, 2.35. $C_{65}H_{64}N_2P_3ZnRu$ requires C, 68.87; H, 5.78; N, 2.47.

Synthesis and characterisation of 13

[Ru(PPh$_3$)$_3$(CO)H$_2$] (20 mg, 0.02 mmol) and ZnPhos (38 mg, 0.06 mmol) were dissolved in C_6D_6 (0.6 mL) in a J. Youngs resealable NMR tube and the sample heated at 80 °C for 5 h. Standing at room temperature, precipitated **13** as a deep-red microcrystalline solid, although always contaminated with traces of PPh$_3$. An alternative approach of concentrating the solution and layering with hexane afforded material which always contained a greater amount of PPh$_3$. Yield: 15 mg (50%). $^{13}C\{^{1}H\}$ NMR: δ_C (126 MHz, C_6D_6, 298 K): 215.5 (m, Ru–*C*O), 174.6 (dt, $J_{C,P}$ = 33 Hz, $J_{C,P}$ = 6 Hz, Ar), 173.6 (d, $J_{C,P}$ = 33 Hz, Ar), 173.2 (d, $J_{C,P}$ = 55 Hz, Ar), 157.9 (dvt, $J_{C,P}$ = 31 Hz, $J_{C,P}$ = 9 Hz, Ar), 146.4 (d, $J_{C,P}$ = 15 Hz, Ar), 146.0 (d, $J_{C,P}$ = 15 Hz, Ar), 144.5 (m, Ar), 143.9 (vt, $J_{C,P}$ = 18 Hz, Ar), 139.2 (s, Ar), 139.1 (s, Ar), 139.0 (s, Ar), 138.8 (s, Ar), 138.4 (d, $J_{C,P}$ = 32 Hz, Ar), 135.4 (d, $J_{C,P}$ = 13 Hz, Ar), 135.1 (vt, $J_{C,P}$ = 6 Hz, Ar), 134.0 (d, $J_{C,P}$ = 17 Hz, Ar), 133.8 (vt, $J_{C,P}$ = 5 Hz, Ar), 133.3 (vt, $J_{C,P}$ = 5 Hz, Ar), 133.0 (d, $J_{C,P}$ = 10 Hz, Ar), 132.4 (vt, $J_{C,P}$ = 5 Hz, Ar),

130.7 (d, $J_{C,P}$ = 5 Hz, Ar), 130.5 (s, Ar), 129.3 (d, $J_{C,P}$ = 8 Hz, Ar), 128.6 (s, Ar), 128.5 (m, Ar), 127.9 (m, Ar), 127.9 (s, Ar), 127.6 (s, Ar), 127.1 (s, Ar), 125.9 (s, Ar), 125.1 (d, $J_{C,P}$ = 3 Hz, Ar). ATR-IR (cm^{-1}): 1896 (ν_{CO}). Elemental analysis was precluded by the contamination with PPh_3 noted above (see Fig. S41†).

Synthesis and characterisation of 14

$[Ru(IMe_4)(PPh_3)_2(CO)H_2]$ (20 mg, 0.026 mmol) and ZnPhos (30 mg, 0.051 mmol) were dissolved in C_6D_6 (0.6 mL) in a J. Youngs resealable NMR tube and the sample heated at 70 °C for 6 h. Upon concentrating and layering with hexane, colourless crystals of **14** were formed. Yield: 7 mg (32%). ^{1}H NMR: δ_H (400 MHz, C_6D_6, 298 K): 8.60 (d, $^3J_{H,H}$ = 7.0 Hz, 2H, Ar), 7.97 (m, 5H, Ar), 7.58 (m, 2H, Ar), 7.12 (t, $^3J_{H,H}$ = 7.6 Hz, 2H, Ar), 7.08–6.94 (m, 9H, Ar), 6.71 (t, $J_{H,H}$ = 7.2 Hz, 2H, Ar), 6.58 (t, $^3J_{H,H}$ = 7.4 Hz, 4H, Ar), 3.05 (s, 3H, NCH_3), 1.69 (s, 3H, NCH_3), 1.32 (s, 3H, NC═CCH_3), 0.94 (s, 3H, NC═CCH_3), −6.63 (td, $^2J_{H,P}$ = 20.9 Hz, $^2J_{H,H}$ = 5.7 Hz, 1H, Ru*H*), −9.65 (td, $^2J_{H,P}$ = 16.7 Hz, $^2J_{H,H}$ = 5.7 Hz, 1H, Ru*H*). ^{31}P{^{1}H} NMR: δ_P (162 MHz, C_6D_6, 298 K): 68.6 (s). ^{13}C{^{1}H} NMR: δ_C (101 MHz, C_6D_6): 207.3 (t, $^2J_{C,P}$ = 8 Hz, Ru–*C*O), 189.0 (t, $^2J_{C,P}$ = 9 Hz, Ru–C_{NHC}), 172.9 (vt, J = 31 Hz, $ZnAr_{Cquat}$), 149.1 (vt, J = 32 Hz, Ar), 140.7 (vt, J = 18 Hz, Ar), 140.4 (vt, J = 18 Hz, Ar), 139.2 (vt, J = 12 Hz, Ar), 139.1 (vt, J = 12 Hz, Ar), 133.0 (m, Ar), 132.5 (vt, J = 5 Hz, Ar), 128.9 (s, Ar), 127.1 (s, Ar), 126.6 (br vt, J = 3 Hz, Ar), 125.0 (m, Ar), 123.5 (s, N*C*H═CHN), 123.3 (s, NCH═*C*HN), 36.7 (s, NCH_3), 35.7 (s, NCH_3), 9.8 (s, H_3CC═CCH_3), 9.3 (s, H_3CC═CCH_3). Elemental analysis. Found: C, 61.00; H, 4.78; N, 3.13. $C_{44}H_{42}N_2OP_2ZnRu$ requires C, 62.67; H, 5.02; N, 3.32. Multiple attempts repeatedly gave low %*C* values.

X-ray crystallography

Data for all structures (Table S2†) were obtained using an Agilent SuperNova instrument and a Cu-Kα source. All experiments were conducted at 150 K and structures were universally solved using SHELXT.[55] Refinements were conducted using SHELXL[56] *via* the Olex2 [57] interface. Convergences were generally straightforward. Where disorder prevailed, appropriate distance and ADP restraints were included, in these regions, to assist convergence. Only additional, noteworthy, points follow. Two independent molecules of the bimetallic complex plus 2.5 molecules of benzene were noted to constitute the asymmetric unit in the structure of **7**. The hydride ligand present in each of the two complexes was located and refined freely. Solvent was manifest as half of an ordered molecule (proximate to a crystallographic inversion centre) and two complete benzene moieties that were treated for 75 : 25 and 57 : 43 disorder, respectively. The hydride was located and refined freely in the structure of **9**. In the structure of **10**, the hydride was also readily located and it was freely refined, but with a riding U_{iso} value. Data for this structure were impacted by sample twinning plus decay of the crystal in the beam, both of which were addressed during integration of the raw frames.

The asymmetric unit in **11** contains one molecule of the bimetallic complex and half of a molecule of hexane. The latter lies proximate to a crystallographic inversion centre, which serves to generate the remainder of the solvent. The hydrides were located and refined without restraints. There is evidence for some smearing of the solvent-electron density, but this precluded any sensible modelling efforts that were trialled.

The asymmetric unit in the structure of **13** was seen host to one molecule of benzene in addition to one molecule of the metal complex. In **14**, the asymmetric unit was seen to contain four independent molecules which are broadly similar. However, the overlay of these four molecules shows that there are significant conformational differences with respect to the positioning of the pendant phenyl rings. All hydrides were located and refined subject to some comparative distance restraints. These separate similarity restraints were applied to the following four, chemically equivalent, sets of bonds (i) Ru4–H7D, Ru3–H5D, Ru1–H1D, Ru2–H3D (ii) Ru2–H4D, Ru1–H2D, Ru4–H8D, Ru3–H6D (iii) Zn2–H3D, Zn1–H1D, Zn4–H7D, Zn3–H5D and (iv) Zn3–H6D, Zn1–H2D, Zn2–H4D, Zn4–H8D. The requirement for restraints reflects the fact that the crystal was not entirely single in nature, but that it did not readily index as a multi-twinned sample either. As a result, the largest unassigned electron density peak is 1.87 electrons per cubic Å, while the largest hole is 3.51 e $Å^{-3}$.

Conflicts of interest

There are no conflicts of interest to declare.

Data availability

The data supporting this article have been included as part of the ESI.† Crystallographic data for **9**, **10**, **11**, **7**, **13**, and **14** have been deposited at the CCDC under accession numbers 2409552, 2409553, 2409554, 2409555, 2409556 and 2409557† and can be obtained from **https://www.ccdc.cam.ac.uk/**.

Acknowledgements

The work was supported by an EPSRC Doctoral Training Award to AMW. We thank Dr Robin Stein (Bruker) for solid-state NMR assistance and Dr David Liptrot for use of his ATR-IR spectrometer. We dedicate this paper to Professor Paul Pringle, on the occasion of his upcoming retirement, in recognition of his many contributions to the chemistry of metal-phosphine complexes.

References

1 J. I. van der Vlugt, *Angew. Chem., Int. Ed.*, 2010, **49**, 252–255.
2 M. A. Bennett, S. K. Bhargava, N. Mirzadeh and S. H. Privér, *Coord. Chem. Rev.*, 2018, **370**, 69–128.
3 G. M. Adams and A. S. Weller, *Coord. Chem. Rev.*, 2018, **355**, 150–172.

4 M. T. Whited, *Dalton Trans.*, 2021, **50**, 16443–16450.
5 Y. H. Lee and B. Morandi, *Coord. Chem. Rev.*, 2019, **386**, 96–118.
6 P. W. N. M. van Leeuwen and P. C. J. Kamer, *Catal. Sci. Technol.*, 2018, **8**, 26–113.
7 M. Vogt and R. Langer, *Eur. J. Inorg. Chem.*, 2020, 3885–3898.
8 M. Sircoglou, M. Mercy, N. Saffon, Y. Coppel, G. Bouhadir, L. Maron and D. Bourissou, *Angew. Chem., Int. Ed.*, 2009, **48**, 3454–3457.
9 A. Amgoune and D. Bourissou, *Chem. Commun.*, 2011, **47**, 859–871.
10 R. C. Cammarota and C. C. Lu, *J. Am. Chem. Soc.*, 2015, **137**, 12486–12489.
11 G. Bouhadir and D. Bourissou, *Struct. Bonding*, 2017, **171**, 141–201.
12 M. V. Vollmer, J. Xie and C. C. Lu, *J. Am. Chem. Soc.*, 2017, **139**, 6570–6573.
13 J. Takaya and N. Iwasawa, *J. Am. Chem. Soc.*, 2017, **139**, 6074–6077.
14 R. C. Cammarota, L. J. Clouston and C. C. Lu, *Coord. Chem. Rev.*, 2017, **334**, 100–111.
15 D. You and F. P. Gabbai, *Trends Chem.*, 2019, **1**, 485–496.
16 J. Takaya, *Chem. Sci.*, 2021, **12**, 1964–1981.
17 P. Steinhoff, R. Steinbock, A. Friedrich, B. G. Schieweck, C. Cremer, K. N. Truong and M. E. Tauchert, *Dalton Trans.*, 2018, **47**, 10439–10442.
18 P. Steinhoff, M. Paul, J. P. Schroers and M. E. Tauchert, *Dalton Trans.*, 2019, **48**, 1017–1022.
19 J. P. Schroers, M. N. Kliemann, J. M. A. Kollath and M. E. Tauchert, *Organometallics*, 2021, **40**, 3893–3906.
20 M. A. Bennett, M. Contel, D. C. R. Hockless and L. L. Welling, *Chem. Commun.*, 1998, 2401–2402.
21 M. A. Bennett, M. Contel, D. C. R. Hockless, L. L. Welling and A. C. Willis, *Inorg. Chem.*, 2002, **41**, 844–855.
22 Y. P. Cai, S. J. Jiang, L. Q. Dong and X. Xu, *Dalton Trans.*, 2022, **51**, 3817–3827.
23 M. García-Melchor, B. Fuentes, A. Lledós, J. A. Casares, G. Ujaque and P. Espinet, *J. Am. Chem. Soc.*, 2011, **133**, 13519–13526.
24 M. V. Polynski and E. A. Pidko, *Catal. Sci. Technol.*, 2019, **9**, 4561–4572.
25 A. M. Messinis, S. L. J. Luckham, P. P. Wells, D. Gianolio, E. K. Gibson, H. M. O'Brien, H. A. Sparkes, S. A. Davis, J. Callison, D. Elorriaga, O. Hernandez-Fajardo and R. B. Bedford, *Nat. Catal.*, 2019, **2**, 123–133.
26 F. M. Miloserdov, C. J. Isaac, M. L. Beck, A. L. Burnage, J. C. B. Farmer, S. A. Macgregor, M. F. Mahon and M. K. Whittlesey, *Inorg. Chem.*, 2020, **59**, 15606–15619.
27 K. Fukuda, T. Harada, N. Iwasawa and J. Takaya, *Dalton Trans.*, 2022, **51**, 7035–7039.
28 S. Burling, M. F. Mahon, B. M. Paine, M. K. Whittlesey and J. M. J. Williams, *Organometallics*, 2004, **23**, 4537–4539.
29 N. Bramananthan, E. Mas-Marzá, F. E. Fernandéz, C. E. Ellul, M. F. Mahon and M. K. Whittlesey, *Eur. J. Inorg. Chem.*, 2012, 2213–2219.
30 B. Cordero, V. Gómez, A. E. Platero-Prats, M. Revés, J. Echeverría, E. Cremades, F. Barragán and S. Alvarez, *Dalton Trans.*, 2008, 2832–2838.
31 P. R. Markies, G. Schat, O. S. Akkerman and F. Bickelhaupt, *Organometallics*, 1990, **9**, 2243–2247.
32 P. E. Garrou, *Chem. Rev.*, 1981, **81**, 229–266.
33 F. Mohr, S. H. Privér, S. K. Bhargava and M. A. Bennett, *Coord. Chem. Rev.*, 2006, **250**, 1851–1888.
34 The major product formed with 2 equivalents of IEt_2Me_2 appeared to be an analogue of the IMes and $I^iPr_2Me_2$ compounds **8** and **9** shown in Scheme 4, based on the similarity of the hydride and ^{31}P NMR resonances shown in Fig. S1 and S2† to those in Fig. S10 and S11† (see also ref. 36). No attempts were made to isolate this species for further characterisation.
35 Repeating the reaction at higher temperature (55–80 °C) or in a different solvent (toluene or THF) failed to generate any more of the proposed isomer. Based on the ^{31}P NMR resonances (Fig. S2;† see also Experimental section), it contains two cyclometallated phosphine ligands *cis* to one another. Recrystallisation of the crude mixture of **7** and the proposed isomer from toluene/hexane at low temperature gave just **7**.
36 F. M. Miloserdov, A.-F. Pécharman, L. Sotorrios, N. A. Rajabi, J. P. Lowe, S. A. Macgregor, M. F. Mahon and M. K. Whittlesey, *Inorg. Chem.*, 2021, **60**, 16256–16265.
37 Again the crystals required manual separation from a colourless solid, assumed to be $(I^iPr_2Me_2)_2ZnMe_2$.
38 A. E. W. Ledger, A. Moreno, C. E. Ellul, M. F. Mahon, P. S. Pregosin, M. K. Whittlesey and J. M. J. Williams, *Inorg. Chem.*, 2010, **49**, 7244–7256.
39 D. Pingen, T. Lebl, M. Lutz, G. S. Nichol, P. C. J. Kamer and D. Vogt, *Organometallics*, 2014, **33**, 2798–2805.
40 J. Alós, T. Bolaño, M. A. Esteruelas, M. Oliván, E. Oñate and M. Valencia, *Inorg. Chem.*, 2014, **53**, 1195–1209.
41 It is unclear whether this degradation is due to the chlorinated solvent itself, or traces of water in the solvent. See also ref. 27.
42 S. B. Duckett, R. J. Mawby and M. G. Partridge, *Chem. Commun.*, 1996, 383–384.
43 H. Samouei, F. M. Miloserdov, E. C. Escudero-Adán and V. V. Grushin, *Organometallics*, 2014, **33**, 7279–7283.
44 L. Bemi, H. C. Clark, J. A. Davies, C. A. Fyfe and R. E. Wasylishen, *J. Am. Chem. Soc.*, 1982, **104**, 438–445.
45 Z. Yan and R. Zhang, *J. Magn. Reson.*, 2023, **357**, 107597.
46 In the low frequency region of the spectrum, there were small changes in chemical shift ($\Delta\delta$ = 0.1–0.2 ppm) for both ZnPhos and PPh_3 resonances over the course of the reaction. This observation shows some similarities to the behaviour of resonances for **13** and PPh_3 as a function of temperature described in the main text.
47 We have reported intramolecular attack of Ru–H on the C–O bond of DPEphos. M. K. Cybulski, N. A. Beattie, S. A. Macgregor, M. F. Mahon and M. K. Whittlesey, *Chem. – Eur. J.*, 2020, **26**, 11141–11145.
48 R. H. Crabtree, *Chem. Rev.*, 2015, **115**, 127–150.

49 R. A. Schunn, E. R. Wonchoba and G. Wilkinson, *Inorg. Synth.*, 1971, **13**, 131–134.
50 N. Ahmad, J. J. Levison, S. D. Robinson and M. F. Uttley, *Inorg. Synth.*, 1974, **15**, 45–48.
51 H. Samouei and V. V. Grushin, *Organometallics*, 2013, **32**, 4440–4443.
52 N. Kuhn and T. Kratz, *Synthesis*, 1993, 561–562.
53 S. Harder, L. Brandsma, J. A. Kanters, A. Duisenberg and J. H. van Lenthe, *J. Organomet. Chem.*, 1991, **420**, 143–154.
54 S. Porcel, G. Bouhadir, N. Saffon, L. Maron and D. Bourissou, *Angew. Chem., Int. Ed.*, 2010, **49**, 6186–6189.
55 G. M. Sheldrick, *Acta Crystallogr., Sect. A: Found. Adv.*, 2015, **71**, 3–8.
56 G. M. Sheldrick, *Acta Crystallogr., Sect. C: Struct. Chem.*, 2015, **71**, 3–8.
57 O. V. Dolomanov, L. J. Bourhis, R. J. Gildea, J. A. K. Howard and H. Puschmann, *J. Appl. Crystallogr.*, 2009, **42**, 339–341.